Journal of Molecular Liquids 286 (2019) 110859

Contents lists available at ScienceDirect

Journal of Molecular Liquids

journal homepage: www.elsevier.com/locate/molliq

Sorption and photocatalytic degradation of methylene blue on bentonite-ZnO-CuO nanocomposite☆

Krzysztof Szostak *, Marcin Banach

Faculty of Chemical Engineering and Technology, Cracow University of Technology, Cracow, Poland

ARTICLE INFO

Article history:
Received 5 April 2018
Received in revised form 21 December 2018
Accepted 24 April 2019
Available online 2 May 2019

Keywords:
Sorption
Photocatalysis
Nanocomposite
Bentonite-ZnO-CuO
Methylene blue
Batch

ABSTRACT

This paper presents a method for removing organic dyes by sorption and photocatalytic processes on a bentonite bed modified with ZnO-CuO nanocomposite. The effect of the initial dye concentration and temperature on the amount of dye removed from the solution was investigated. The results obtained at equilibrium state allowed us to determine the equilibrium and kinetic models and the thermodynamic parameters for the studied processes. The Langmuir isotherm is the best model for describing the equilibrium processes for both sorption and sorption with photocatalysis. In terms of kinetics, both processes are accurately described by the pseudo-second order model, which demonstrates the chemical nature of sorption. Due to the negative ΔG values calculated from the tests, it was found that the studied processes are spontaneous. It was possible to obtain a better degree of purification of the dye solution using combined sorption and photocatalysis compared to the sorption process itself.

1. Introduction

Due to the widespread use of dyes in many industries, enormous amounts of waste water are contaminated by colorants that have a negative impact on the aquatic environment and are difficult to be removed with conventional methods. Even small quantities of dyes in aquatic environments are strongly visible and adversely affect the ecosystem, limiting the access to sunlight, hindering the free growth of fauna and flora. Dyes are relatively poorly biodegradable substances, which can cause the accumulation of these pollutants in the environment. It should also be noted that some dyes can be toxic or carcinogenic. The complex chemical structure and diversity of colouring compounds make them difficult to remove and make the basic methods used in waste water treatment plants less effective. For this reason, it is important to look for modern methods for dye removal that could be based on natural or waste materials [1].

Among the various methods used for dye removal, one of the most popular are sorption techniques which are considered as simple to implement and not requiring a lot of investment. The most popular sorbents are activated carbons, but due to the high costs of production and regeneration, natural or waste products are sought [2]. It has been found that plant and animal substances such as lignin [3], chitin and chitosan [4] or peat [5], as well as mineral substances including fly ash [6], bauxite and kaolinite [7] dolomite [8] or bentonite [9], have been used as sorbents for dye removal. The last mentioned bentonite was chosen as the bed base used in the study because of its favourable sorption properties, environmental friendliness and easy availability. Thanks to its packet structure, bentonite has high CEC (Cation Exchange Capacity) value and is physically and chemically resistant [10].

One of the alternatives for sorption are photocatalytic processes. They are considered modern techniques which in combination with traditional methods, can give us desired results in terms of efficiency and safety. They are regarded as waste-free, which can additionally use the natural source of energy as sun rays. Application of UV-radiated catalytic processes can also be used to decrease the temperature of the process in compare with traditional processes which reduces the total amount of energy that needs to be delivered to the process [11]. Currently the most popular material used in photocatalytic processes is TiO_2, which is also widely used in its nanoparticle form due to its improved photocatalytic properties. It is also used in combination with other materials, such as multiwalled carbon nanotubes in order to achieve material photocatalytically active under visible light irradiation [12]. Another material successfully used in photocatalysis is ZnO in nanoparticle form. The advantages of nanosized zinc oxide are environmental stability, and low cost when compared with other nanoparticle oxides. The main problem with similar zinc and titanium oxides is high band width value of about 3.2–3.3 eV which means it can absorb only in the UV region. To overcome these drawbacks, researchers have concentrated their studies on mixed oxide semiconductors. Effective separation of charges can be

☆ This research did not receive any specific grant from funding agencies in the public, commercial, or not-for-profit sector.

* Corresponding author at: Faculty of Chemical Engineering and Technology, Institute of Chemistry and Inorganic Technology, Cracow University of Technology, Warszawska 24, Cracow 31-155, Poland.
E-mail address: kszostak@chemia.pk.edu.pl (K. Szostak).

https://doi.org/10.1016/j.molliq.2019.04.136
0167-7322/

achieved by coupling two or more semiconductor particles with different energy levels and thereby increasing the efficiency of the photocatalytic activity by the vector transfer of photogenerated electrons and electron holes from one semiconductor to another (Fig. 1) [13]. Researchers have been able to successfully receive coupled semiconductor materials such as ZnO-CuO (5%wt CuO) [13,14], CuO-TiO_2 (up to 4%wt CuO) [15,16], WO_3-TiO_2 [17], ZnO-TiO_2 (up to 1:1 wt ratio) [18], ZnO-SnO_2 (molar ratio of 2:1 and 1:1) [19], TiO_2-MgO (up to 10%wt MgO) [20], or SnO_2-ZnO (molar ratio of 1:1) [21].

New sorption materials with additional functionalities are sought after. Nanomaterials and nanocomposites are now widely studied. Of course, they are expensive compared to traditional materials, but they are used in much smaller quantities. The aim of this work was to develop a novel sorption bed based on bentonite mixed with nanosized zinc oxide and doped with nanosized copper oxide, which could be used to photocatalytic removal of microorganic impurities from aqueous solutions and to determine the parameters of sorption and sorption processes with simultaneous photocatalysis. In this particular system, nano-CuO acts as a sensitizer to the whole material where electrons transfered from the valence band to the conduction band leaves positive holes in valence band. After separation of these species, the dissolved oxygen (O^2) will react with photo-induced electrons to form an oxidative radical ($\cdot O_2^-$). The direct transfer of photo-induced holes from ZnO to CuO takes place in ZnO-CuO nanocomposites, which leads to oxidation of hydroxyl (OH^-) ions to hydroxyl radicals ($\cdot OH$) through photo-induced holes [23,24]. In order to better understanding the mechanisms and effects of the nanocomposite bed, determining of the parameters of equilibrium, kinetics and thermodynamics of the studied processes is of great importance. In addition, by providing information on the mechanisms and stability, this work is included in the generally accepted concept of green chemistry [24–26].

An example of the application of materials obtained in this work are coating materials obtained on the basis of paint and plaster, in which only 2.5% addition of the obtained nanocomposite contributed to give photocatalytic properties to the obtained coatings. Such coating materials are currently a very popular topic both scientifically and industrially, due to the multiplicity of their applications, and should be thoroughly tested.

2. Materials and methods

Methylene blue (POCH), zinc nitrate (Aldrich), copper nitrate (Aldrich) and sodium hydroxide (POCH) used in present studies were of analytical reagent grade. All aqueous solutions were prepared using high purity deionized water.

2.1. Synthesis of bentonite-ZnO-CuO nanocomposite

The bed synthesis was carried out in a laboratory pressure reactor Bench Top Reactor 4525 with volume of 1 dm^3 by Parr Instruments.

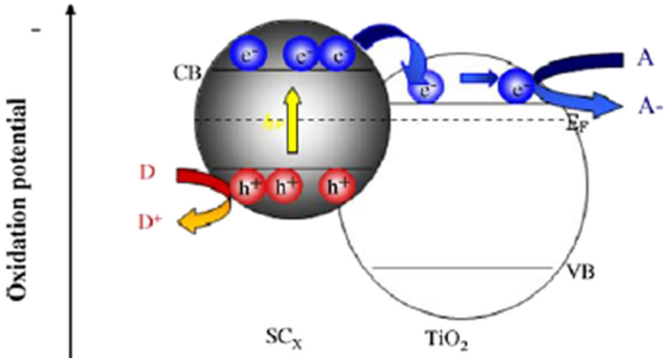

Fig. 1. Mechanism of vector electron transfer from semiconductor to TiO_2 [22].

The amount of reactants was adjusted to obtain a bed with a mass ratios of bentonite:ZnO:CuO = 1:1:0.04.

Here, 1.35 g of bentonite, 180 cm^3 of 0.1 mol/dm^3 $Zn(NO_3)_2$ solution and 20 cm^3 of 2 mol/dm^3 NaOH solution were used for the synthesis of bentonite-ZnO nanocomposite. The reaction was carried out with continuous stirring for 30 min after reaching the temperature of 200 °C. The maximum pressure achieved in the reactor was 14 bar. After the time elapsed, the reaction mixture was cooled to room temperature and then the filtrate was dried at 70 °C for 24 h. Finally, 2.77 g of material was obtained which was used as substrate for further synthesis.

Here, 2.77 g of bentonite-ZnO nanocomposite, 7.3 cm^3 of $CuSO_4$ 0.1 mol/dm^3 solution, 0.81 cm^3 of NaOH solution 2 mol/dm^3 and 192 cm^3 of deionized water to complete the reaction mixture to a volume of 200 cm^3 were used to obtain the bentonite-ZnO-CuO nanocomposite. The synthesis was carried out analogously to the method described above. The resulting bed was dried and then calcinated in an electric furnace for 2 h at 400 °C. Bed samples were analysed by SEM-EDS, BET, FTIR, and XRD.

2.2. Sorption and photocatalysis processes

Approximately 25 mg of bed and 50 cm^3 of methylene blue with concentrations of 20, 40, 60, 80, and 100 mg/dm^3 were used to study the kinetics and balance of sorption processes. The sorption process was carried out in batch mode for 1, 3, 5, 10, 20, and 30 min for each concentration. The processes were carried out in closed containers while protecting the samples against access to outside light. The photocatalysis studies were performed analogously; however, the containers were open and additionally exposed to UV light at a wavelength of 366 nm. Analogously to the above, processes were conducted to determine the thermodynamic parameters of sorption processes. The processes were carried out at temperatures of 20, 30, 40, 50, 60, and 70 °C, for the highest concentration i.e. 100 mg/dm^3 and the longest time, i.e. 30 min. The resulting suspensions were filtered and the solutions were subjected to UV-VIS spectrophotometric analysis to determine the dye concentration. In addition, deposits after sorption and photocatalysis processes were subjected to SEM-EDS and FTIR analyses.

According to the following equations the sorption capacity at a given time (qt) and at the state of equilibrium (qe) and the distribution coefficient (Kd, cm^3/g) for this studies was determined [27].

$$q_t = \frac{(C_0 - C_t)}{w} \cdot V$$

$$q_e = \frac{(C_0 - C_e)}{w} \cdot V$$

$$K_d = \frac{(C_0 - C_e)}{C_e} \cdot \frac{V}{w}$$

where:

q_t – weight of adsorbed methylene blue at time "t" (mg/g).
q_e – weight of adsorbed methylene blue at equilibrium (mg/g).
C_0 – initial concentration of methylene blue (mg/dm^3).
C_t – concentration of methylene blue at time "t" (mg/dm^3).
C_e – concentration of methylene blue at equilibrium (mg/dm^3).
V – volume of solution (dm^3).
w – bed weight used in the sorption process (g).
K_d – distribution coeficient (cm^3/g).

2.2.1. Sorption equilibrium

Equilibrium parameters for methylene blue were modelled according to the following sorption models: Langmuir, Freundlich, Temkin, and Dubinin-Radushkevich.

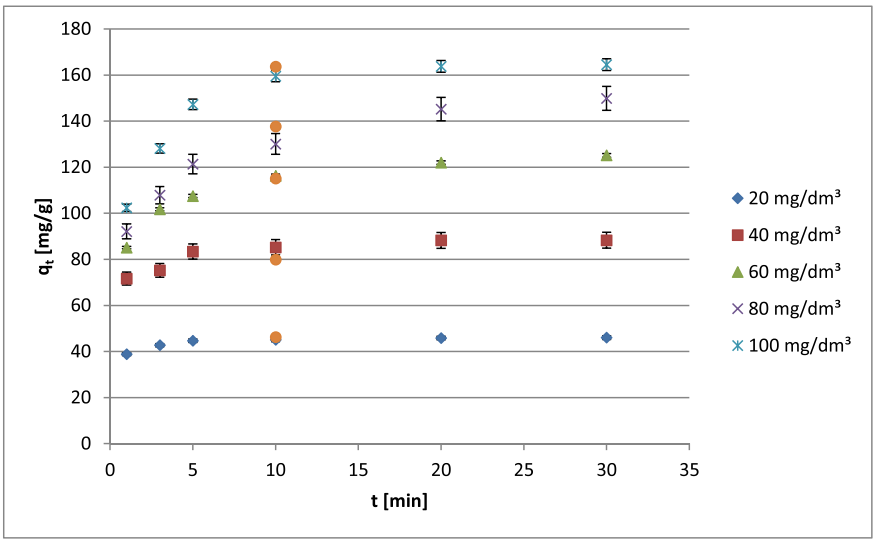

Fig. 2. Sorption of methylene blue on the bentonite-ZnO-CuO bed at different times and at different initial concentrations (at room temperature).

2.2.1.1. Langmuir isotherm. Langmuir's isotherm describes the formation of monolayer on the adsorbent surface, while the adsorption of subsequent layers does not take place. In this way, the Langmuir model represents the distribution of the ion balance between solid and liquid phases. This isotherm applies to monolayer adsorption on a surface containing a finite number of identical sites. Langmuir isotherm is determined by the following equation [28]:

$$\frac{C_e}{q_e} = \frac{C_e}{q_{max}} + \frac{1}{K_L \cdot q_{max}}$$

where:

q_e – sorption capacity at equilibrium (mg/g).
q_{max} – maximum sorption capacity (mg/g).
K_L – Langmuir constant (dm^3/mg).

Based on the Langmuir model, a separation factor (R_L) can be calculated from which it can be determined whether the sorption process is favourable or unfavorable.

$$R_L = \frac{1}{1 + K_L C_0}$$

where:

$R_L = 0$ - the sorption process is irreversible,
$0 < R_L < 1$ - conditions are favourable for sorption.
$R_L = 1$ - linear nature of sorption.
$R_L > 1$ - unfavorable conditions for sorption.

2.2.1.2. Freundlich isotherm. Freundlich isotherm describes the sorption properties of heterogeneous surfaces. It can be assumed that the sorption process is imperfect, reversible, and multilayer. The model is represented by the equation [27]:

$$\log q_e = \log K_F + \frac{1}{n} \log C_e$$

where:

q_e - mass of adsorbed methylene blue at equilibrium (mg/g).
K_F - Freundlich constant ($mg^{1-(1/n)}(dm^3)^{1/n}g^{-1}$).
n - heterogeneity parameter.

2.2.1.3. Temkin isotherm. The Temkin model describes monolayer adsorption on a heterogeneous surface. This isotherm corresponds to continuous energy distribution of adsorption sites where no minimal or maximum energy limitations apply. Interaction between the sorbate and the sorbent cause the decrease in the heat of adsorption to be linear rather than logarithmic. Temkin isotherm is represented by the following equation [29]:

$$q_e = B \ln K_t + B \ln C_e$$

$$B = \frac{RT}{b_t}$$

where:

K_t - constant associated with maximal binding energy (dm^3/g).
B - heat related sorption constant (J/mol).
R - gas constant (8.314 Jmol/K).
T - temperature (K).
B_t - Temkin constant.

2.2.1.4. Dubinin-Radushkevich isotherm. This model summarizes the adsorption process occurring on heterogeneous surfaces. Dubinin-

Table 1
Equilibrium parameters and equations of methylene blue sorption onto bentonite-ZnO-CuO bed.

Isothermic model	Parameters and equations			
Langmuir	Equation	R^2	q_{max} (mg/g)	K_L (dm^3/mg)
	y = 0.0060x + 0.0020	0.9991	166.11	3.0025
Freundlich	Equation	R^2	K_F ($mg^{1(1/n)}(dm^3)^{1/n}g^{-1}$)	1/n
	y = 0.1448x + 2.0453	0.9938	110.99	0.1448
Temkin	Equation	R^2	K_T (dm^3/g)	B
	y = 13.3605x + 120.24	0.9820	8100.36	13.3605
D-R	Equation	R^2	E (J/mol)	q_d (mg/g)
	y = −0.0001x + 4.9926	0.9598	77.38	147.3190

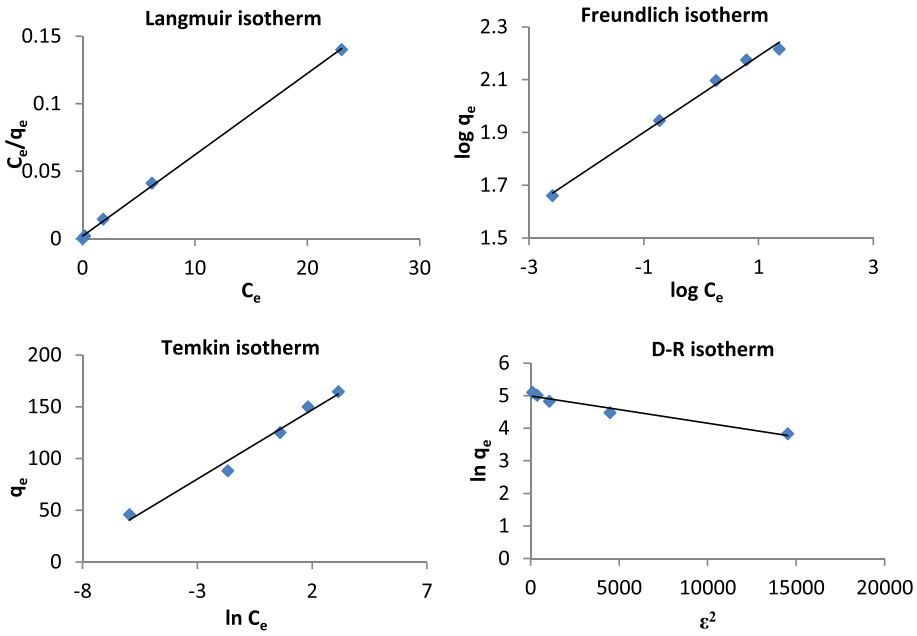

Fig. 3. Linear graphs of different sorption isotherms for methylene blue on a bentonite-ZnO-CuO bed.

Radushkevich isotherm model can be described by the equation [27]:

$$\ln q_e = \ln q_d - (B_d\varepsilon^2)$$
$$\varepsilon = RT\ln\left(1+\frac{1}{C_e}\right)$$

where:

q_d - theoretical maximum saturation potential of isotherm (mg/g).
B_d - constant D-R isotherms associated with sorption energy (mol^2/J^2).
ε - Polanyi adsorption potential.

The average amount of sorption energy can tell whether it is physical or chemical character of sorption.

$$E = \frac{1}{\sqrt{2B_d}}$$

where:

E - average sorption energy (J/mol).

2.2.2. Sorption kinetics

2.2.2.1. Pseudo-first-order equation. In the kinetic model designed in accordance with the pseudo-first order equation, shown below, the reaction rate is directly proportional to the difference between the equilibrium concentration and the instantaneous concentration of the adsorbate in the solid phase [30]:

$$\frac{dq_t}{dt} = k_1(q-q_t)$$

The pseudo-first order linear equation is as follow s:

$$\log(q_e-q_t) = \log q_e - \frac{k_1}{2,303}t$$

where:
q_t - amount of adsorbed substance in time "t" (mg/g).
q_e - adsorption capacity at equilibrium (mg/g).
k_1 - constant for model (1/min).
t - time (min).

2.2.2.2. Pseudo-second-order equation. In the kinetic model of the pseudo-second order equation, the overall rate of sorption is proportional to the square of the driving force [28]:

$$\frac{dq_t}{dt} = k_2(q-q_t)^2$$

The pseudo-second order linear equation is as follows:

$$\frac{t}{q_t} = \frac{1}{k_2q_e^2} + \frac{1}{q_e}$$

where:

q_t - amount of adsorbed substance in time "t" (mg/g).
q_e - adsorption capacity at equilibrium (mg/g).

Table 2
Parameters of kinetic models for methylene blue sorption on bentonite-ZnO-CuO bed.

Kinetic model	Methylene blue concentration (mg/dm^3)				
	20	40	60	80	100
Pseudo-first order					
q_e	5.7214	27.1957	36.7959	62.3736	65.7506
k_1	0.1861	0.2821	0.1280	0.1283	0.2328
R^2	0.9416	0.9669	0.9772	0.9891	0.9874
Pseudo-second order					
q_e	46.2963	89.2857	128.2051	153.8462	169.4915
k_2	0.09720	0.02727	0.009813	0.005152	0.008095
R^2	1.0000	0.9999	0.9997	0.9987	0.9999
Elovich					
α	132.76	455.41	1083.62	1599.78	2153.01
β	0.4941	0.1878	0.08549	0.05729	0.05314
R^2	0.8732	0.9217	0.9845	0.9932	0.9229
Intramolecular diffusion					
I	39.871	70.882	85.048	86.548	106.21
K_{id}	1.3272	3.6922	8.152	12.570	12.631
R^2	0.6858	0.8094	0.8731	0.9405	0.7591

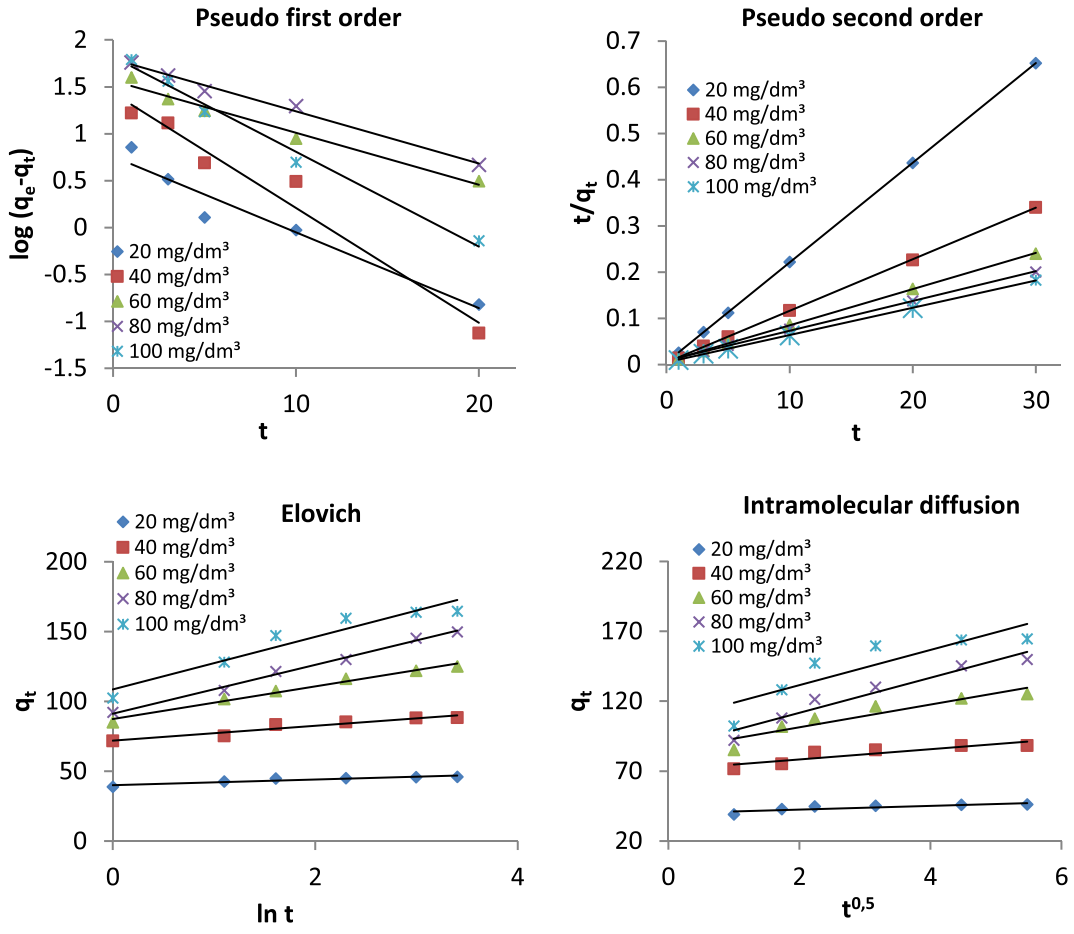

Fig. 4. Line graphs of different kinetic models for methylene blue on bentonite-ZnO-CuO bed.

k_2 - constant for model (g/mg · dm³/min).
t - time (min).

2.2.2.3. Elovich model. One of the most popular heterogeneous kinetic equations describing the adsorption of gases on solids is the Elovich model. The model assumes multilayer adsorption and an exponential increase in the number of active sites in the sorption range. This model is described by the equation [27]:

$$q_t = \frac{1}{\beta}\ln(\alpha\cdot\beta) + \frac{1}{\beta}\ln(t)$$

where

α - initial sorption rate (mg/g·min).
β - desorption constant (g/mg).

The α value is a constant related to chemisorption rate and β is a constant which depicts the extent of surface coverage. They are associated with the surface coverage degree and energy activation for adsorption.

2.2.2.4. Intra-molecular diffusion model. Intra-molecular diffusion refers to the molecules diffusing from the solution to the solid phase. It describes adsorption onto porous adsorbents in highly stirred systems. The equation for this model is shown below [28]:

$$q_t = k_{id}t^{0,5} + I$$

where:
k_{id} - constant intra-molecular diffusion (mg/g·min^{0,5}).
I - factor related to mass transfer by boundary layers.

2.2.3. Sorption thermodynamics

Designated thermodynamic parameters were used to determine the spontaneity of the sorption process. Using the van't Hoff equation, the change in the Gibbs free energy (ΔG) was calculated from the formula below.

$$\Delta G = -RTlnK_d$$

while change in standard enthalpy (ΔH) and change in standard entropy (ΔS) are then obtained from the linear plot of $\ln K_d$ versus 1/T with following equation [31]:

$$\ln K_d = -\frac{\Delta H}{RT} + \frac{\Delta S}{R}$$

where:

R - gas constant 8.314 (J/mol·K).
T - temperature (K).

Table 3
Thermodynamic parameters for methylene blue sorption on bentonite-ZnO-CuO bed.

T (K)	ΔH (J/mol)	ΔS (J/mol·K)	ΔG (J/mol)
293	−23.24	27.80	−7812
303			−8167
313			−8534
323	283.80	20.43	−8612
333			−8325
343			−8353

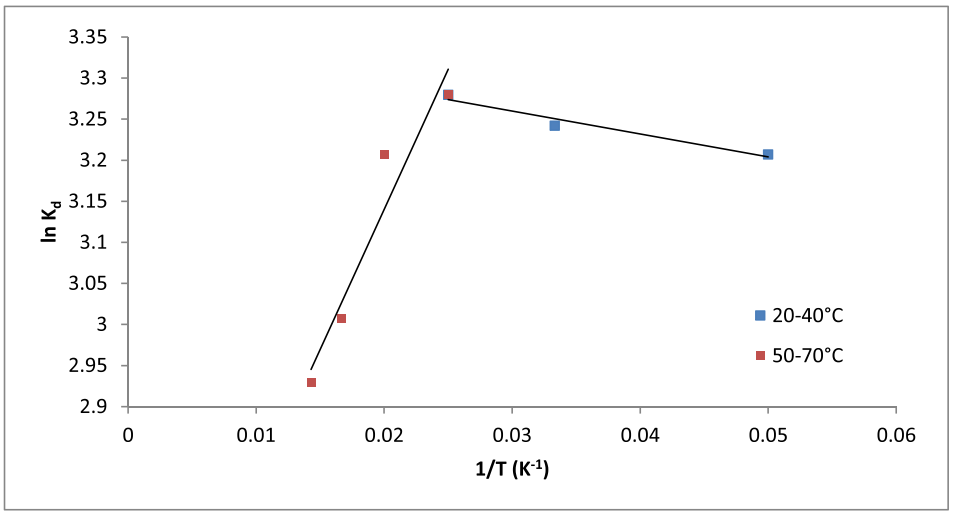

Fig. 5. Graph of lnKd dependence from 1/T to determine thermodynamic parameters for methylene blue sorption processes (C = 100 mg/dm3, t = 30 min).

ΔG - change in Gibbs free energy (J/mol).
ΔH - change in standard enthalpy (J/mol).
ΔS - change in standard entropy (J/mol).

2.3. Methods

The main method used in this work to determine the concentration of methylene blue in aqueous solutions was UV-VIS spectroscopy. Analyses were carried out by measuring the absorbance of methylene blue aqueous solutions at 664 nm on a Rayleigh UV-1800 apparatus. SEM-EDS analysis was performed to examine the surface area of the received deposit on the 1430VP LEO by Electron Microscopy Ltd. In order to study chemical bonds present in the sorbent, FTIR analysis was used via a Nicolet 380 spectrometer. The phase composition of received bed was examined by XRD analysis using an X'Pert Philips diffractometer equipped with a PW 1752–1700 graphite monochromator. BET analysis was used to determine the surface area and both the size and distribution of pores in used sorption material. BET measurements were performed on the ASAP 2010 from Micromeritics using nitrogen at 77 K as adsorbed gas.

3. Results and discussion

3.1. Sorption processes

3.1.1. Influence of the contact time and the initial concentration on dye removal

The effect of time on the sorption process and the effect of the initial concentration on the total sorption capacity of the bed has been carried out (Fig. 2). As seen, both the increase in time and increase in initial concentration resulted in an increase in the total capacity of the bed. It can also be said that the state of equilibrium was reached after 20 min.

3.1.2. Equilibrium studies

In order to determine the parameters of equilibrium, the sorption process was carried out for various time periods, and with different initial concentrations. Equilibrium parameters were determined for the Langmuir, Freundlich, Temkin and Dubinin-Raduszkiewicz sorption models (Table 1, Fig. 3).

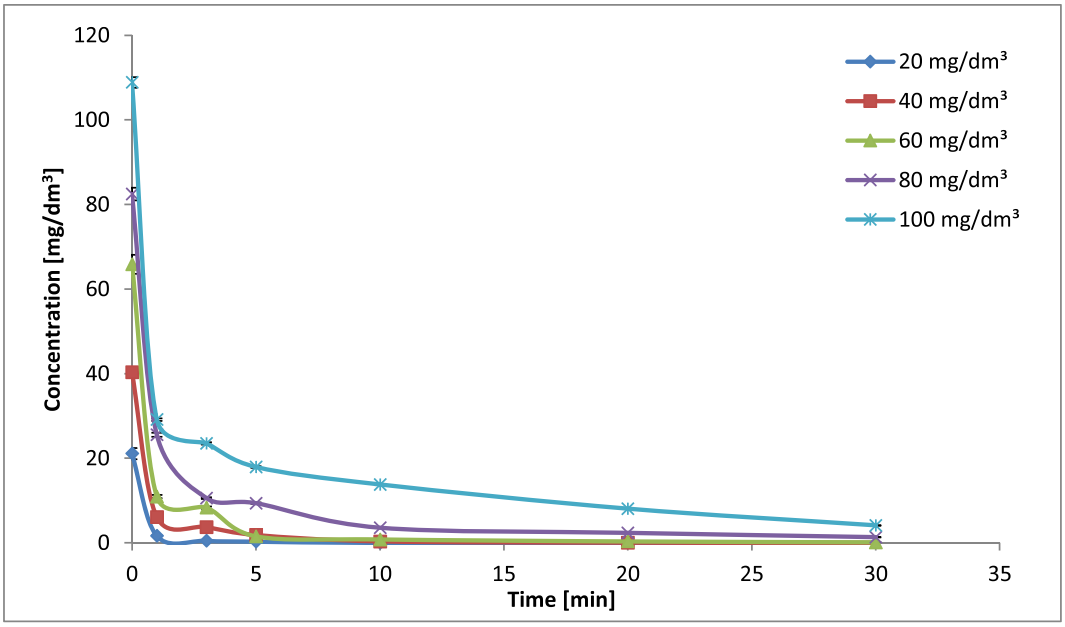

Fig. 6. Dependence of methylene blue concentration according to the time of photocatalysis and initial concentration.

Table 4
Parameters and equations of isotherms of sorption processes during photocatalysis of methylene blue on bentonite-ZnO-CuO bed.

Isothermic model	Parameters and equations			
Langmuir	**Equation**	**R^2**	**q_{max} (mg/g)**	**K_L (dm^3/mg)**
	$y = 0.0048\times + 0.0005$	0.9913	208.33	9.6001
Freundlich	**Equation**	**R^2**	**K_F ($mg^{1(1/n)}(dm^3)^{1/n}g^{-1}$)**	**1/n**
	$y = 0.1895\times + 2.2230$	0.9113	167.11	0.1895
Temkin	**Equation**	**R^2**	**K_T (dm^3/g)**	**B**
	$y = 20.2604\times + 170.8886$	0.9714	4603.68	20.2604
D-R	**Equation**	**R^2**	**E (J/mol)**	**q_d (mg/g)**
	$y = -0.0001\times + 5.3899$	0.9290	70.71	219.1815

The best model describing the methylene blue sorption processes on bentonite doped with zinc and copper oxides is Langmuir isotherm having the highest R^2, which indicates a monolayer type of sorption. It means that the whole surface has identical adsorption activity. In other words the binding energy on the entire surface is uniform. This also indicates a negligible interaction between the dye molecules adsorbed on the surface. In addition, the nanocomposite used has a finite surface area, and hence a sorption capacity, which is why the sorption process can be better described the Langmuir model.

The second highest value of the coefficient was obtained for the Freundlich model which has a good fit at low initial concentrations, however, shows deviations at high concentration values. This may be due to the fact that at low concentrations, the sorption process may follow the Freundlich model which assumes an exponentially increasing adsorption, however at higher concentrations the entire surface of the bed can covered, which causes the model to diverge [32]. Despite the high R^2 coefficients of the other models, Langmuir isotherm proved to be the best-fitted model showing the smallest deviations of the designated model from linearity throughout the range of concentrations.

The data collected indicate that the R_L was always greater than zero and <1, indicating that the sorption process was in favourable conditions [33].

Vadivelan, and Kumar from Anna University in Chennai, India, carried out batch type process of sorption of methylene blue onto rice husk particles. Their results show that sorption of MB onto ruse husk is best fitted by Langmuir isotherm with correlation coefficient value of 0.984986, which confirms the monolayer coverage of MB onto rice husk particles. Maximum sorption capacity in their study was found to be 40.5833 mg/g, which is comparable with other low cost adsorbents, but at the same time it is four times worse than q_{max} achieved in this study [34].

3.1.3. Kinetic modelling

One of the most important parameters influencing the efficiency of sorption is the time of the process. In order to investigate the effect of time and kinetic parameters of the process, the methylene blue sorption was carried out similarly to that in the determination of equilibrium parameters, i.e. for different time periods and at different initial

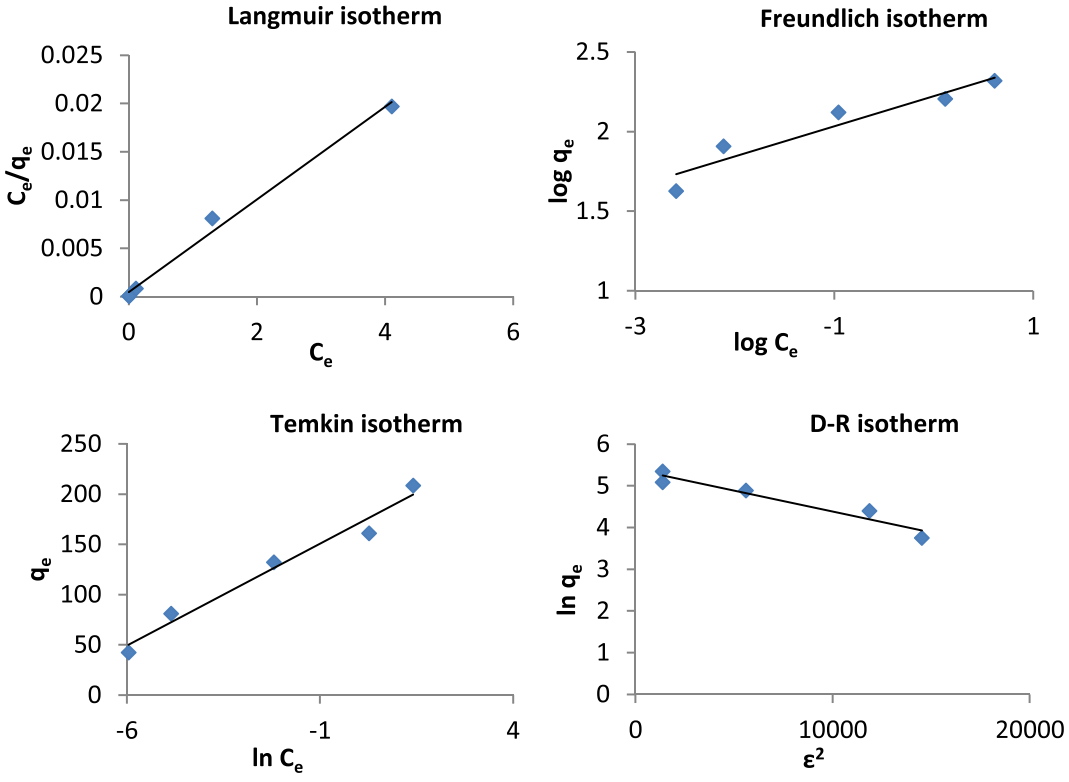

Fig. 7. Isotherms for sorption processes during photocatalysis of methylene blue on bentonite-ZnO-CuO bed.

Table 5
Parameters of kinetic models for methylene blue photocatalysis on bentonite-ZnO-CuO bed.

Kinetic Model	Methylene blue concentration (mg/dm^3)				
	20	40	60	80	100
Pseudo-first order					
q_e	3.0024	14.0637	21.9887	73.8924	46.6337
k_1	0.2262	0.2524	0.2153	0.3669	0.09281
R^2	0.9440	0.9730	0.9399	0.9764	0.9787
Pseudo-second order					
q_e	42.5532	81.9672	133.3333	163.9344	212.7660
k_2	0.2301	0.04651	0.02679	0.01378	0.006694
R^2	1.0000	1.0000	0.9999	0.9999	0.9992
Elovich					
α	107.25	348.68	924.85	1724.49	2388.05
β	0.9998	0.2575	0.1375	0.07678	0.07176
R^2	0.8096	0.9211	0.8709	0.8730	0.9881
Intramolecular diffusion					
I	39.42	68.87	109.99	121.65	155.40
K_{id}	0.6415	2.6269	4.8692	8.5502	10.1550
R^2	0.6080	0.7696	0.7122	0.6869	0.9580

concentrations of the dye. For the investigation of kinetic parameters, pseudo-first order, pseudo-second order, Elovich, and intra-molecular diffusion models were used (Table 2, Fig. 4).

The above results allow the direct comparison and discussion of several kinetic models. In order to compare these models in terms of lead time and initial concentration, the determinant R^2 based on the linear equations was used. From the above graphs in Fig. 4 and data in Table 2, the most suitable kinetic model of this process is the pseudo-second order model, which has the highest R^2 coefficients at all initial concentrations. This demonstrates the presence of the chemical character of sorption.

Bulut and Aydin from Uniwersity of Dicle in Diyarbakir, Turkey studied kinetics of methylene blue sorption onto wheat shells obtaining the same results as in this study. Their research also lead to conclusion that this process is confirmed by pseudo-second order kinetics due to the determined correlation coefficients >0.99 for this particular kinetic model [35].

3.1.4. Thermodynamic studies

Temperature is of great importance in research into sorption processes. It affects the sorption process in two ways. First, it lowers the viscosity of the solution, and secondly it increases particle mobility in solution, thus causing a change in methylene blue sorption equilibrium. That is why the temperature impact studies on the methylene blue sorption process have been carried out to determine the basic thermodynamic parameters of the process.

Thermodynamic parameters were tested for a period of 30 min at an initial concentration of 100 mg/dm^3 at a variable temperature (Table 3, Fig. 5).

The calculated negative ΔG values indicate that the methylene blue sorption process on the bentonite-ZnO-CuO bed is a spontaneous process. Within the range of 20–40 °C, there is an exothermic reaction due to the negative enthalpy of the reaction, whereas in the range 50–70 °C the enthalpy is positive, which means that the reaction is endothermic in this range. Such change could be the result of the surface complexation variations that occurs as adsorption temperature is modified [36]. It is also possible to notice the decrease in ΔG along with the increase in temperature, which indicates a decrease in the driving force of the process, which in turn results in less adsorption. Positive values of ΔS show the affinity of methylene blue to the test bed and increased randomness during the adsorption process [33].

Hong et al. from Wuhan University in Wuhan, China, studied thermodynamics of methylene blue sorption onto pure bentonite in which

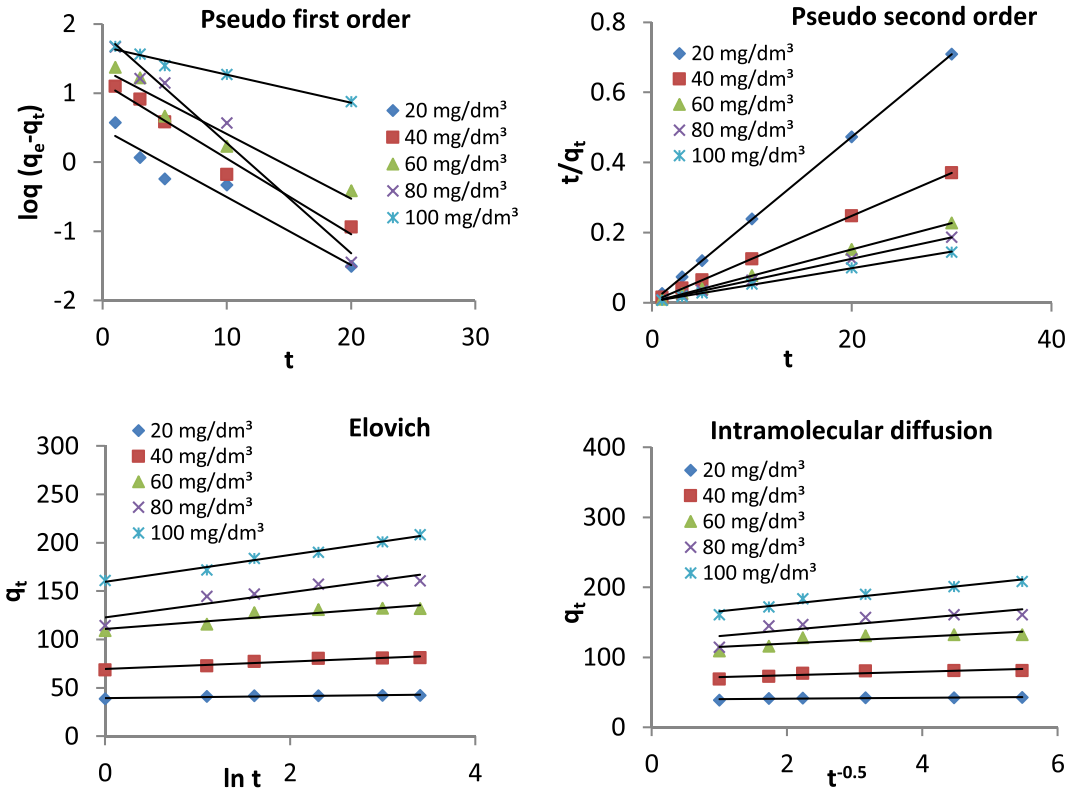

Fig. 8. Line graphs of kinetic models for sorption processes during photocatalytic purification of methylene blue on bentonite-ZnO-CuO bed.

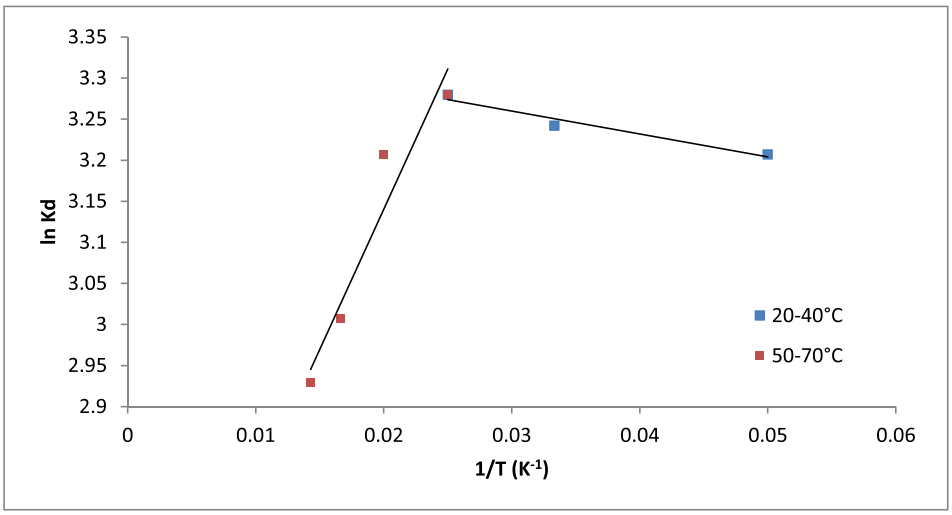

Fig. 9. Graph of lnKd from 1/T to determine thermodynamic parameters for photocatalytic of methylene blue (C = 100 mg/dm3, t = 30 min).

Table 6
Thermodynamic parameters of the sorption process with simultaneous photocatalysis.

T (K)	ΔH (J/mol)	ΔS (J/mol·K)	ΔG (J/mol)
293	−153.43	33.23	−7487
303			−8518
313			−8264
323	222.13	20.90	−8456
333			−8093
343			−8149

ΔG values decreased from −17.0 to −19.4 kJ/mol which clearly shows that the adsorption process of MB on bentonite becomes more favourable at higher temperatures. They got positive value of ΔH, which shows that reaction was endothermic. They also reported a positive value of ΔS, meaning increasing randomness at the solid/liquid interface during the process, and affinity of MB to bentonite [37].

3.2. Sorption processes with simultaneous photocatalysis

3.2.1. Influence of the contact time and the initial concentration on dye removal

As with sorption, the effect of time and initial concentration on the efficiency of the process was investigated (Fig. 6). Time significantly influences the degree of methylene blue removal. From the graph it can be read that for the highest concentration over time the dye concentration decreases systematically, even after 20 min, while the sorption process

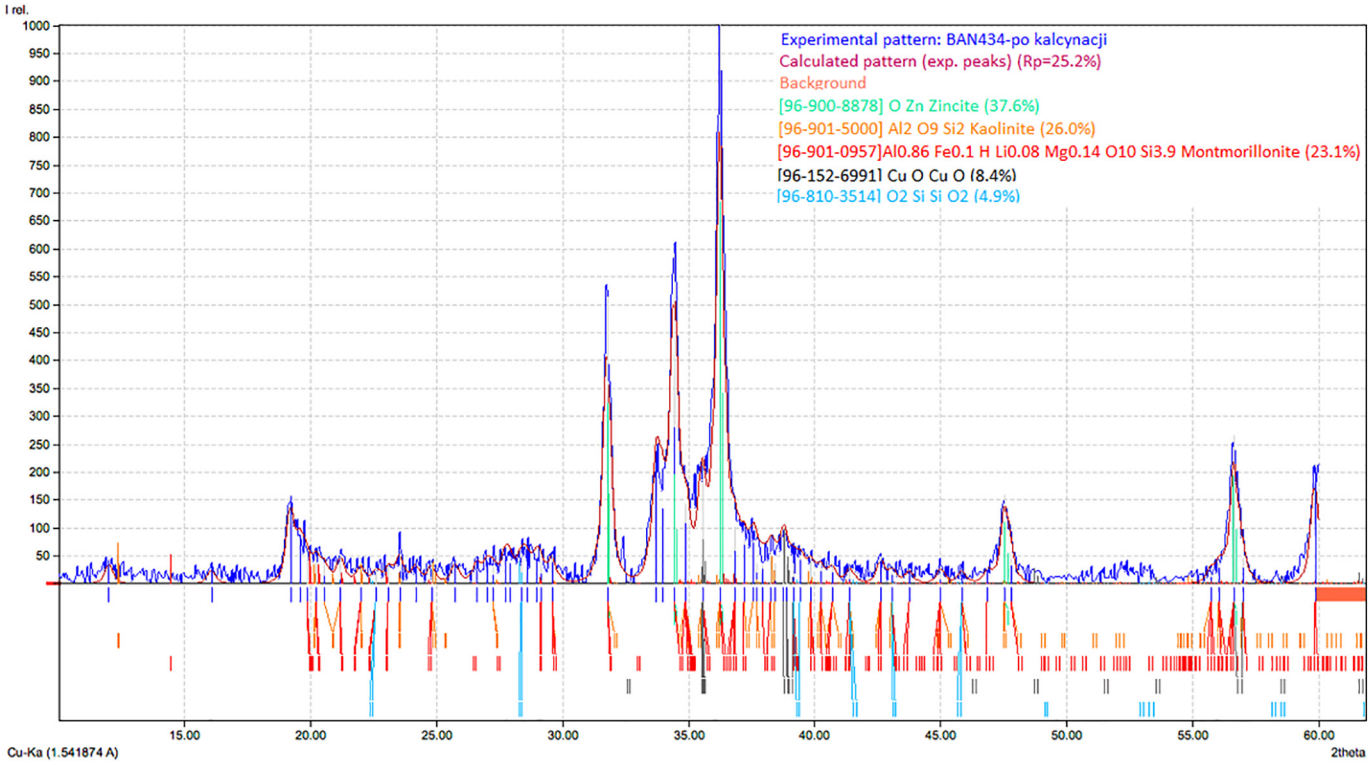

Fig. 10. XRD diffraction of the bed.

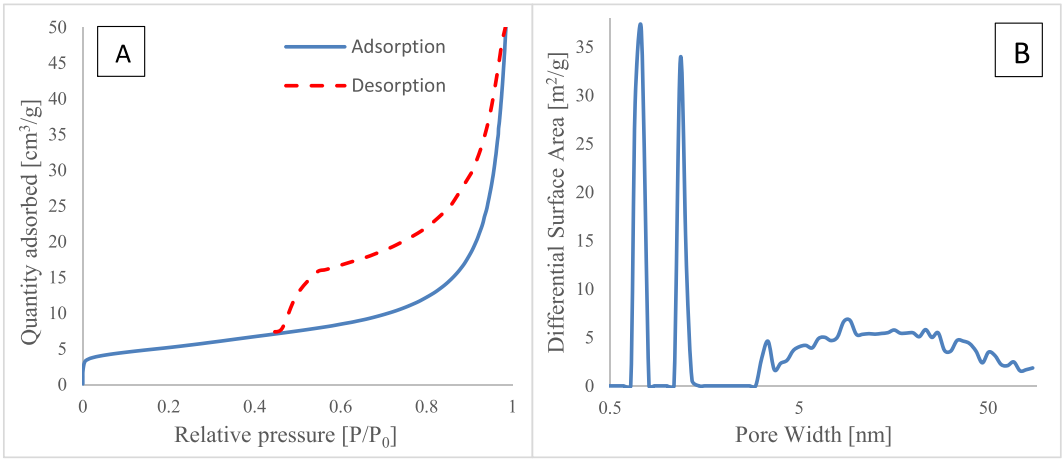

Fig. 11. A - Adsorption and desorption isotherms determined by the BET method, B - pore distribution represented by the differential surface.

after such time has already reached equilibrium. This is due to the continuous dye decomposition in photocatalytic processes.

3.2.2. Equilibrium studies

Equilibrium parameters of sorption processes with simultaneous photocatalysis were calculated for Langmuir, Freundlich, Temkin and Dubinin-Raduszkiewicz models (Table 4, Fig. 7).

From the results summarised in Table 4, it can be concluded that the Langmuir isotherm model based on the highest R^2 coefficient is the best model describing the sorption process during the photocatalytic decomposition of methylene blue on bentonite-ZnO-CuO nanocomposite, which, as previously stated, indicates uniform and monolayered chemical nature of the studied sorption process.

The distribution coefficient always lies between 0 and 1, indicating that the process was under favourable conditions [33].

In comparison with the plain sorption process, the sorption process with simultaneous photocatalysis is characterised by higher values of q_{max} which indicates higher degree of removal. The difference in the amount of dye removed from solution is due to appearance of photocatalytic degradation. Nonetheless Langmuir isotherm is the best suited equilibrium model for both processes.

3.2.3. Kinetic modelling

As for the kinetic parameters for sorption during photocatalysis, pseudo-first order, pseudo-second order, Elovich and intra-molecular diffusion models were used (Table 5, Fig. 8).

A kinetic model for the determination of sorption processes occurring during the photocatalytic purification of methylene blue by the test bed was shown to be a pseudo-second order model. This is due to the highest R^2 ratios for all initial concentrations. As can be seen in the chart, the graphical representation of this model has an almost linear form, which demonstrates the perfect fit of the model to this process. This demonstrates the chemical nature of sorption in this process.

Both sorption and sorption with simultaneous photocatalysis process are described by pseudo-second order kinetic model. Although combined processes have higher R^2 values than classical sorption processes, this indicates better fit of the model to the process under investigation. Also, the q_{max} parameter has a higher value when looking at the highest concentration (100 mg/dm^3) for combined photocatalytic-

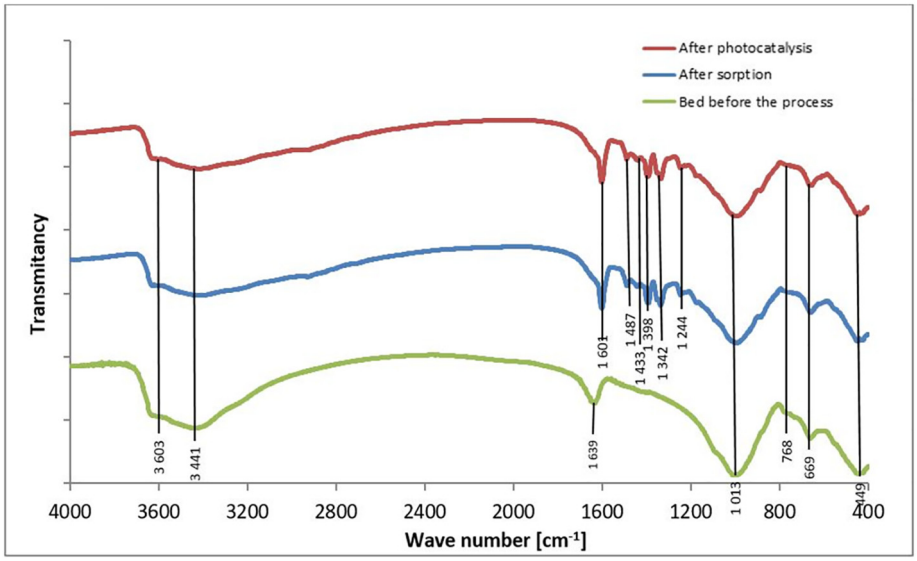

Fig. 12. Comparison of FTIR analysis results for pure bed, bed after sorption (10 min, C = 40 mg/dm^3) and post-photocatalytic bed (10 min, C = 40 mg/dm^3).

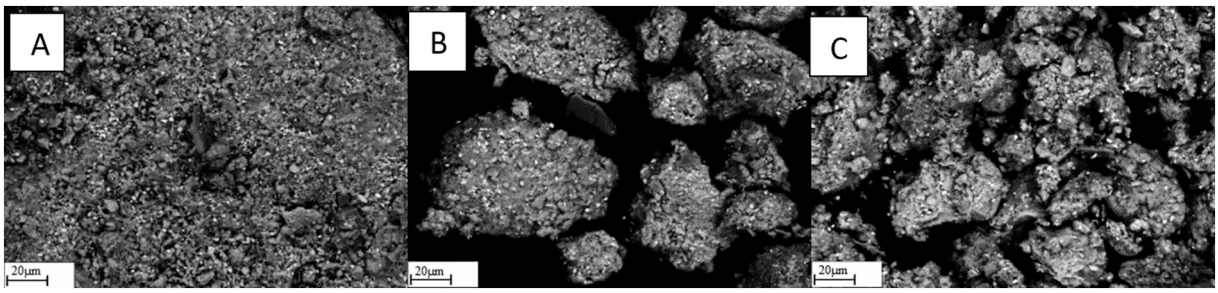

Fig. 13. Images of SEM analysis, A – pure bed, B – deposit after sorption (t = 10 min, C = 40 mg/dm^3), C - deposit after photocatalysis (t = 10 min, C = 40 mg/dm^3).

sorption process than sorption itself. It shows that photodegradation is occurring during the process.

3.2.4. Thermodynamic studies

The linear relationship of lnKd from 1/T has been prepared (Fig. 9), while the calculated thermodynamic parameters are given in Table 6.

All calculated values of ΔG are less than zero, which proves the spontaneity of processes. This values are also quite similar to that reported for the sorption process itself. The negative enthalpy of the reaction in the temperature range of 20–30 °C, says that the process in this temperature range is exothermic, the same as it was in classic sorption process. In the range 40–70 °C, the enthalpy is positive, which indicates the course of endothermic reaction in that range, which was the same in the sorption process described earlier. The change in enthalpy that appears with increasing temperature may be a consequence of surface complexation variations that result from modification of the adsorption temperature [36]. As well as in the case of classic sorption, we can observe a positive values of ΔS, which indicates an increase in the measure of disorder of the system.

Soltani et al. from University Putra Malaysia in Serdang, Malaysia, carried out studies into the degradation of MB under visible light in the presence of ZnS and CdS nanoparticles. They came to the conclusion that higher degradation efficiency and reaction rate can be achieved by increasing the amount of photocatalyst and initial pH value. Also, the mass composition 1:4 of ZnS:CdS in their studies was the most efficient in terms of degradation of MB [38].

3.3. Characterisation of the bed and post-processes deposits

The XRD analysis of the bed (Fig. 10) showed the presence of both zinc oxide and copper oxide which confirms successful execution of the bed. The graph also shows the presence of structures such as SiO_2, montmorillonite and kaolinite, derived from bentonite. The ZnO reflections are sharp and intense, which shows its orderly crystalline form, while a large number of low counts visible on the diffractogram are characteristic of amorphous substances.

BET analysis showed total surface area of 18.33 m^2/g. In addition, the analysis showed a total pore volume of 0.0669 cm^3/g and a total pore area of 12.95 m^2/g. On the graph we can see the hysteresis loop, which with respect to IUPAC classification is a type H3 hysteresis loop (Fig. 11A). It is a typical adsorption loop for non-polar gases on montmorillonite. The H3 loop does not have a flat portion at high p/p_0 values, but instead there is no adsorption limit in this range. This is observed in adsorbents containing platelet aggregates, resulting in slit pores [39]. IUPAC pore classification, in relation to their size, determines micropores up to 2 nm in diameter, mesopores in the range of 2–50 nm and macropores of >50 nm in diameter [40]. According to this classification, we can find the presence of all types of pores in our material (Fig. 11B). It should also be noted that micropores in spite of their small dimensions have a huge impact on the total surface area of the material.

FTIR analyses were performed for pure bed and deposits after sorption and photocatalysis processes carried out for 10 min in methylene blue solutions at 40 mg/dm^3 (Fig. 12). These analyses were conducted to compare the deposit before and after the process. To this end, the suspensions were filtered and the deposits were dried at 105 °C for 24 h and samples were prepared for the aforementioned analyses. The band at 446 cm^{-1} is characteristic for metal oxygen connections. It is triggered by the presence of copper and zinc oxides. The next visible signal at 662 cm^{-1} comes from the combined Al—O and Si—O vibrations. The delicate band present at 774 cm^{-1} denotes the presence of quartz admixtures. The strong signal visible at the 1000 cm^{-1} is characteristic of Si-O-Si tetrahedral groups. The band at 1634 cm^{-1} is derived from H-OH stretching vibrations in water molecules between packages, while these at 3440 cm^{-1} and 3601 cm^{-1} are derived, respectively, from vibrations of hydroxyl groups adsorbed on the surface and Si-OH tensile vibrations [41]. The principal differences between these spectra are the signals occurring in the spectra of bed after the sorption process and the bed after sorption with photocatalysis, with wave numbers of 1244, 1342, 1398, 1433, 1487 and 1601 cm^{-1}. They are characteristic for methylene blue groups (based on MB spectrum [42]) that could adsorb on the surface of the test bed. Confirmation of this hypothesis is the absence of these signals in the pure bed spectrum, which means that the change had to occur during sorption and sorption with photocatalysis. On both spectra of post-process deposits, there is no band seen at 1639 cm^{-1} in the pure bed, which comes from the H-OH stretching of the water molecules between the bentonite packages. It should also be noted that despite the dynamic sorption and photocatalytic processes in all 3 spectra, Me-O bands at 449 cm^{-1}, Al—O and Si—O vibration signals at 669 cm^{-1} as well as quartz admixtures signal at 768 cm^{-1} are still visible, which tells of the continuous presence of applied oxides on the test beds and proves the stability of the deposit.

SEM-EDS analysis was also subjected to pure bed and post-process deposits (Figs. 13, 14). They show white ZnO particles present on the beds whose size oscillates in the area of several nm. It is possible to observe a uniform distribution of zinc oxide on the bentonite surface. The EDS diagrams for sorption and photocatalysis show the presence of sulphur and chlorine that are not present in the pure bed results (Fig. 14). The reason for this is the presence of these elements in the construction of methylene blue, which confirms its adsorption on the surface of the bed. The appearance of elements such as magnesium, aluminium, iron, silicon, potassium and calcium is related to their occurrence in the bentonite structure. Also mapping of these deposits were made (Figs. 15, 16, 17), where uniform distribution of zinc (Figs. 15K, 16K, 17K) and copper (Fig. 15J, 16J, 17J) can be seen, which means that the bed is physically stable during the dynamic process.

4. Conclusions

The synthesis and characterisation of the properties of bentonite bed modified with ZnO-CuO nanoparticles was carried out. The obtained bed can be successfully used in sorption processes as well as photodegradation of methylene blue. Studies into the sorption and photocatalysis of methylene blue on the obtained bed have been carried out, which resulted in determining the most favourable equilibrium, kinetic and thermodynamic models of the processes. Photodegradation of

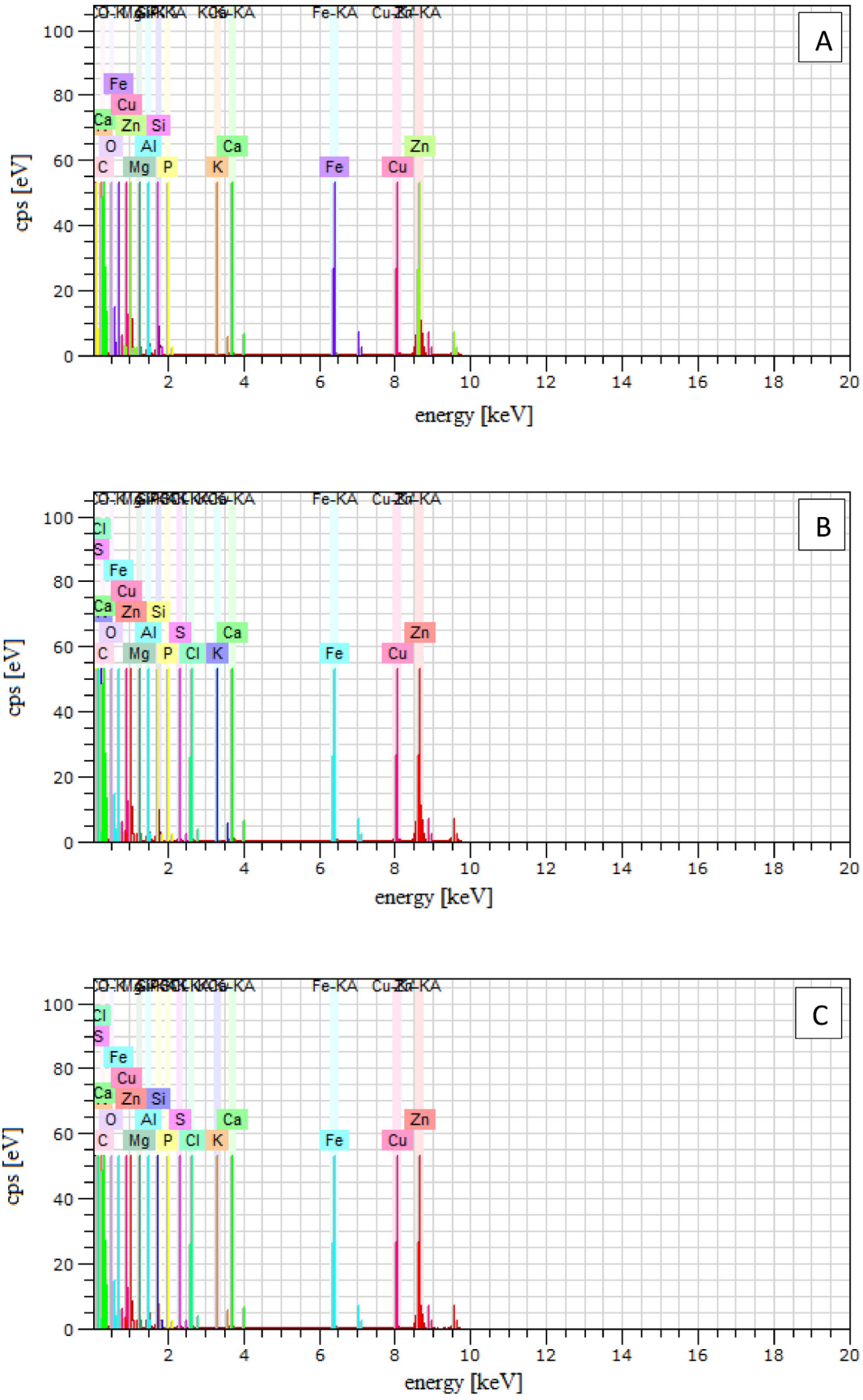

Fig. 14. A - EDS elemental analysis for pure bed, B - EDS elemental analysis of the bed after sorption (t = 10 min, C = 40 mg/dm^3), C - EDS elemental analysis of the bed after photocatalysis (t = 10 min, C = 40 mg/dm^3).

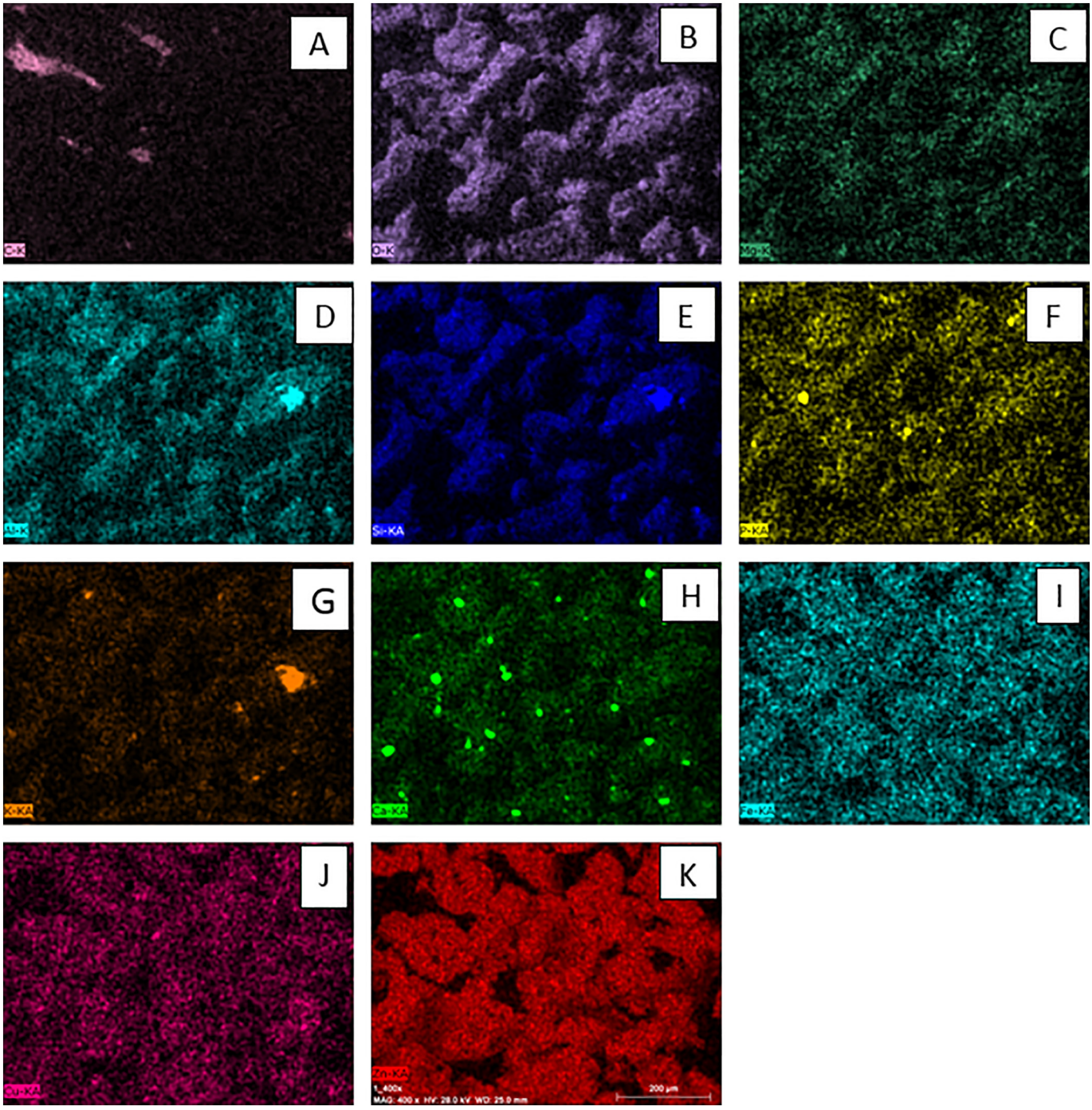

Fig. 15. Mapping of the pure bed.

MB onto ZnO-CuO modified bentonite bed shows that this bed can be used in sorption and photocatalytic degradation of organic compounds from wastewater.

Among the four equilibrium models studied, the best suited for both studied processes is the Langmuir isotherm model, achieving highest R^2 coefficient. In the basis on the separation factor (RL), which values are in the range of 0–1, it can be concluded that both processes were carried out under favourable conditions. Among the four investigated kinetic models, best suited to the sorption process as well as to the sorption with simultaneous photocatalysis was the pseudo-second order model. The methylene blue sorption process on obtained bed as well as sorption under UV irradiation is a spontaneous process that is exothermic in lower temperature range, but changes to endothermic process in higher temperatures. This change in the thermodynamics of the processes may be the result of surface complexation variations that occur with that occur with the temperature change of the adsorption process. Calculated negative values of free enthalpy for both studied processes prove that adsorption is spontaneous process. The combined sorption and photocatalysis process allowed to achieve a better degree of dye removal from the solution reaching higher q_{max} values. The difference in the amount of dye removed from the solution in both processes is due to appearance of photocatalytic degradation under UV light irradiation.

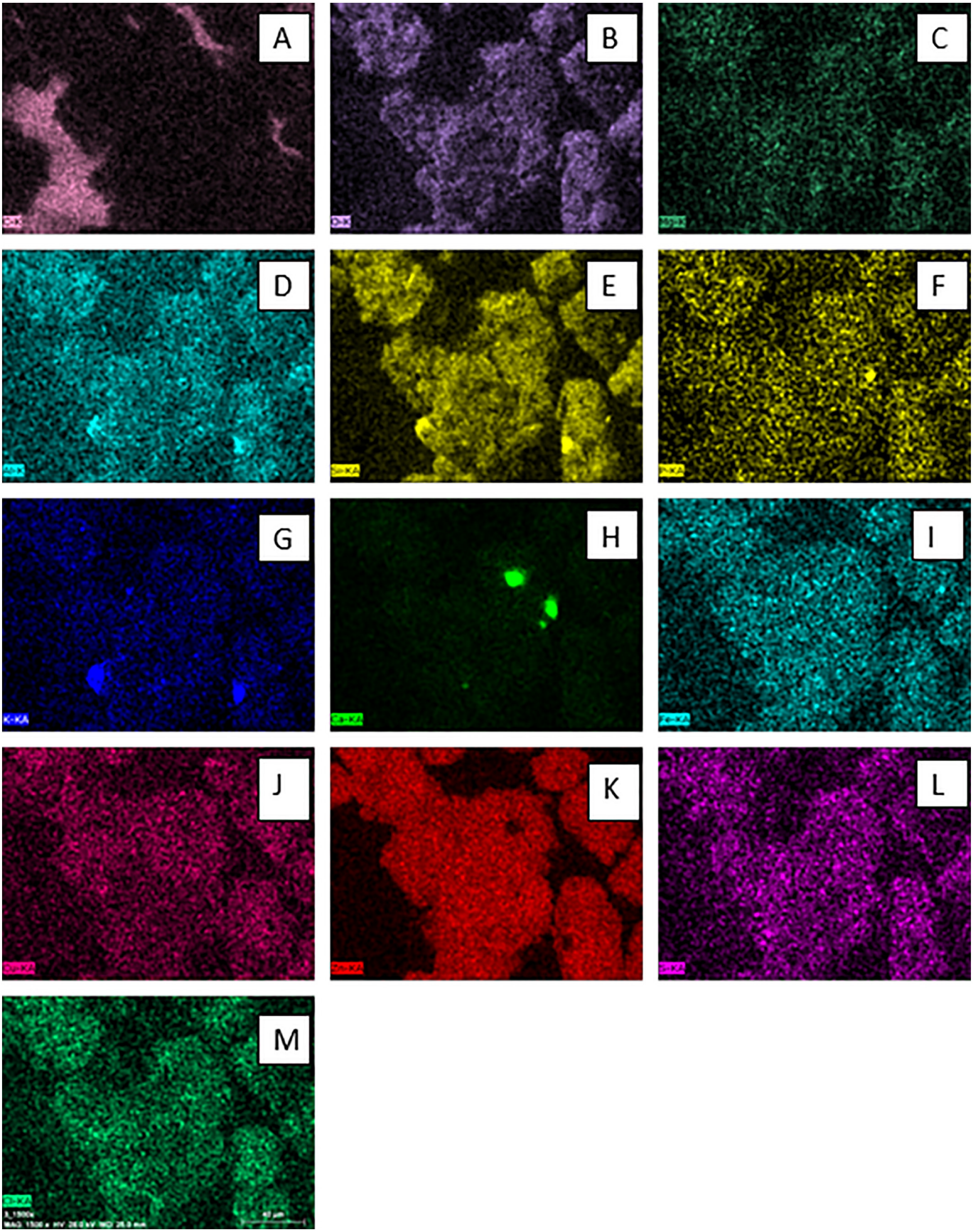

Fig. 16. Mapping of the deposit after the sorption process (t = 10 min, C = 40 mg/dm^3).

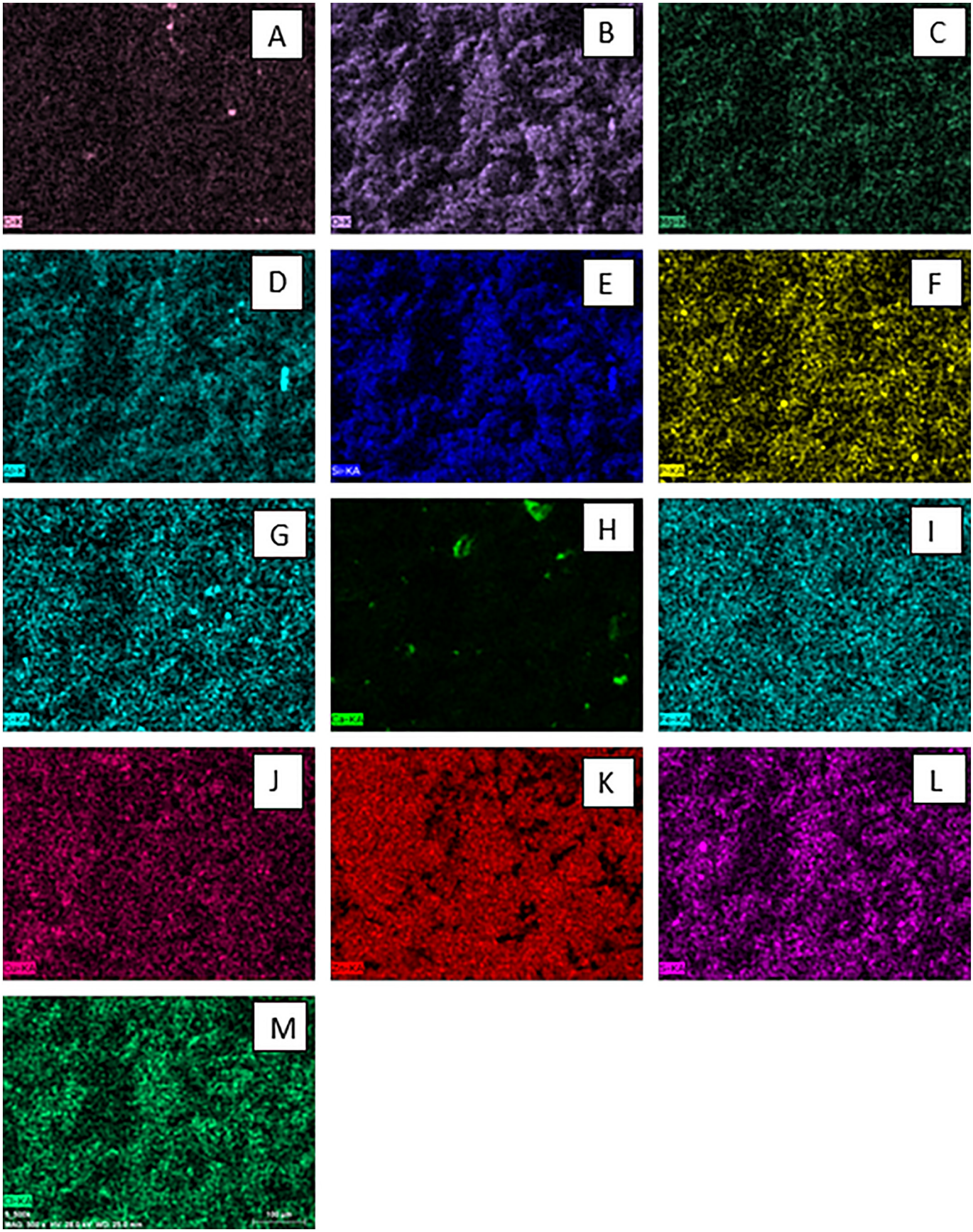

Fig. 17. Mapping of the deposit after the photocatalytic process (t = 10 min, C = 40 mg/dm^3).

Conflict of interest

The authors report no declarations of interest.

References

[1] S. Arora, Textile dyes: It's impact on environment and its treatment, J. Bioremediation Biodegrad. 05 (2014) 6199, https://doi.org/10.4172/2155-6199.1000e146.

[2] P.K. Malik, Dye removal from wastewater using activated carbon developed from sawdust: adsorption equilibrium and kinetics, J. Hazard. Mater. 113 (2004) 81–88, https://doi.org/10.1016/j.jhazmat.2004.05.022.

[3] J. Łebek, W. Wardas, Adsorption of some textile dyes on post-vanillin lignin during its precipitation, Cellul. Chem. Technol. 30 (1996) 212–221.

[4] U. Filipkowska, Efficiency of black DN adsorption onto chitin in an air-lift reactor, Polish J. Environ. Stud. (2004)https://doi.org/10.1109/LRA.2017.2737486.

[5] Y.S. Ho, G. McKay, Sorption of dye from aqueous solution by peat, Chem. Eng. J. (1998)https://doi.org/10.1016/S1385-8947(98)00076-X.

[6] P. Pengthamkeerati, T. Satapanajaru, N. Chatsatapattayakul, P. Chairattanamanokorn, N. Sananwai, Alkaline treatment of biomass fly ash for reactive dye removal from aqueous solution, Desalination (2010)https://doi.org/10.1016/j.desal.2010.05.050.

[7] S.D. Lambert, N.J.D. Graham, C.J. Sollars, G.D. Fowler, Evaluation of inorganic adsorbents for the removal of problematic textile dyes and pesticides, Water Sci. Technol. (1997)https://doi.org/10.1016/S0273-1223(97)00385-5.

[8] G.M. Walker, L. Hansen, J.A. Hanna, S.J. Allen, Kinetics of a reactive dye adsorption onto dolomitic sorbents, Water Res. (2003)https://doi.org/10.1016/S0043-1354(02)00540-7.

[9] S. Al-Asheh, F. Banat, L. Abu-Aitah, The removal of methylene blue dye from aqueous solutions using activated and non-activated bentonites, Adsorpt. Sci. Technol. 21 (2003) 451–462, https://doi.org/10.1260/026361703769645780.

[10] D. Zhao, S. Chen, S. Yang, X. Yang, S. Yang, Investigation of the sorption behavior of Cd(II) on GMZ bentonite as affected by solution chemistry, Chem. Eng. J. (2011) https://doi.org/10.1016/j.cej.2010.11.092.

[11] B.I. Kharisov, U. Ortiz Mendez, J. Rivera de la Rosa, Low-temperature synthesis of phthalocyanine and its metal complexes, Russ. J. Coord. Chem. (2006)https://doi.org/10.1134/S1070328406090016.

[12] D. Zhao, X. Yang, C. Chen, X. Wang, Enhanced photocatalytic degradation of methylene blue on multiwalled carbon nanotubes-TiO_2, J. Colloid Interface Sci. 398 (2013) 234–239, https://doi.org/10.1016/j.jcis.2013.02.017.

[13] R. Saravanan, S. Karthikeyan, V.K. Gupta, G. Sekaran, V. Narayanan, A. Stephen, Enhanced photocatalytic activity of ZnO/CuO nanocomposite for the degradation of textile dye on visible light illumination, Mater. Sci. Eng. C. 33 (2013) 91–98, https://doi.org/10.1016/j.msec.2012.08.011.

[14] S. Das, V.C. Srivastava, Hierarchical nanostructured ZnO-CuO nanocomposite and its photocatalytic activity, J. Nano Res. (2015)https://doi.org/10.4028/www.scientific.net/JNanoR.35.21.

[15] Z. Liu, C. Zhou, Improved photocatalytic activity of nano CuO-incorporated TiO2granules prepared by spray drying, Prog. Nat. Sci. Mater. Int. (2015)https://doi.org/10.1016/j.pnsc.2015.07.005.

[16] G. Li, N.M. Dimitrijevic, L. Chen, T. Rajh, K.A. Gray, Role of surface/interfacial Cu^{2+} sites in the photocatalytic activity of coupled CuO-TiO_2 nanocomposites, J. Phys. Chem. C (2008)https://doi.org/10.1021/jp8068392.

[17] Y. He, Z. Wu, L. Fu, C. Li, Y. Miao, L. Cao, H. Fan, B. Zou, Photochromism and size effect of WO_3 and WO_3-TiO_2 aqueous sol, Chem. Mater. (2003)https://doi.org/10.1021/cm034116g.

[18] G. Marcì, V. Augugliaro, M.J. López-Muñoz, C. Martín, L. Palmisano, V. Rives, M. Schiavello, R.J.D. Tilley, A.M. Venezia, Preparation characterization and photocatalytic activity of polycrystalline ZnO/TiO_2 systems. 2. Surface, bulk characterization, and 4-nitrophenol photodegradation in liquid−solid regime, J. Phys. Chem. B (2001)https://doi.org/10.1021/jp003173j.

[19] W. Cun, Z. Jincai, W. Xinming, M. Bixian, S. Guoying, P. Ping'an, F. Jiamo, Preparation, characterization and photocatalytic activity of nano-sized ZnO/SnO_2 coupled photocatalysts, Appl. Catal. B Environ. (2002)https://doi.org/10.1016/S0926-3373(02)00115-7.

[20] J. Bandara, S.S. Kuruppu, U.W. Pradeep, The promoting effect of MgO layer in sensitized photodegradation of colorants on TiO_2/MgO composite oxide, Colloids Surf. A Physicochem. Eng. Asp. (2006)https://doi.org/10.1016/j.colsurfa.2005.10.059.

[21] L. Zheng, Y. Zheng, C. Chen, Y. Zhan, X. Lin, Q. Zheng, K. Wei, J. Zhu, Network structured SnO2/ZnO heterojunction nanocatalyst with high photocatalytic activity, Inorg. Chem. (2009)https://doi.org/10.1021/ic802293p.

[22] Y. Bessekhouad, D. Robert, J.V. Weber, Photocatalytic activity of Cu2O/TiO2, Bi_2O_3/TiO_2 and $ZnMn_2O_4$/TiO_2 heterojunctions, in: Catal. Today (2005)https://doi.org/10.1016/j.cattod.2005.03.038.

[23] T. Chang, Z. Li, G. Yun, Y. Jia, H. Yang, Enhanced photocatalytic activity of ZnO/CuO nanocomposites synthesized by hydrothermal method, Nano-Micro Lett. (2013) https://doi.org/10.1007/BF03353746.

[24] D.X. Martínez Vargas, J. Rivera De la Rosa, C.J. Lucio-Ortiz, A. Hernández-Ramirez, G.A. Flores-Escamilla, C.D. Garcia, Photocatalytic degradation of trichloroethylene in a continuous annular reactor using Cu-doped TiO_2 catalysts by sol-gel synthesis, Appl. Catal. B Environ. (2015)https://doi.org/10.1016/j.apcatb.2015.05.019.

[25] F. Sánchez-De La Torre, J. Rivera De La Rosa, B.I. Kharisov, C.J. Lucio-Ortiz, Preparation and characterization of cu and ni on alumina supports and their use in the synthesis of low-temperature metal-phthalocyanine using a parallel-plate reactor, Materials (Basel) (2013)https://doi.org/10.3390/ma6104324.

[26] G.L. Dimas-Rivera, J.R. de la Rosa, C.J. Lucio-Ortiz, J.A. de los Reyes Heredia, V.G. González, T. Hernández, Desorption of furfural from bimetallic pt-fe oxides/alumina catalysts, Materials (Basel) (2014)https://doi.org/10.3390/ma7010527.

[27] P. Staroń, J. Chwastowski, M. Banach, Sorption and desorption studies on silver ions from aqueous solution by coconut fiber, J. Clean. Prod. (2017)https://doi.org/10.1016/j.jclepro.2017.02.116.

[28] D.A.O. Langmuir, Temkin Freundlich, Dubinin-Radushkevich, Isotherms studies of equilibrium sorption of Zn^{2+} unto phosphoric acid modified rice husk, IOSR J. Appl. Chem. (2012)https://doi.org/10.9790/5736-0313845.

[29] M. Banach, A. Bukała, J. Pulit-Prociak, P. Staroń, Equilibrium and kinetics of Nanosilver sorption from aqueous solutions, J. Nanosci. Nanotechnol. 16 (2016) 7898–7909, https://doi.org/10.1166/jnn.2016.12753.

[30] L. Chen, D. Zhao, S. Chen, X. Wang, C. Chen, One-step fabrication of amino functionalized magnetic graphene oxide composite for uranium(VI) removal, J. Colloid Interface Sci. 472 (2016) 99–107, https://doi.org/10.1016/j.jcis.2016.03.044.

[31] D. Zhao, L. Chen, M. Xu, S. Feng, Y. Ding, M. Wakeel, N.S. Alharbi, C. Chen, Amino siloxane oligomer modified graphene oxide composite for the efficient capture of U (VI) and Eu(III) from aqueous solution, ACS Sustain. Chem. Eng. 5 (2017) 10290–10297, https://doi.org/10.1021/acssuschemeng.7b02316.

[32] D. Zhao, X. Yang, H. Zhang, C. Chen, X. Wang, Effect of environmental conditions on Pb(II) adsorption on β-MnO_2, Chem. Eng. J. 164 (2010) 49–55, https://doi.org/10.1016/j.cej.2010.08.014.

[33] R. Tang, C. Dai, C. Li, W. Liu, S. Gao, C. Wang, Removal of methylene blue from aqueous solution using agricultural residue walnut Shell: equilibrium, kinetic, and thermodynamic studies, J. Chem. 2017 (2017)https://doi.org/10.1155/2017/8404965.

[34] V. Vadivelan, K. Vasanth Kumar, Equilibrium, kinetics, mechanism, and process design for the sorption of methylene blue onto rice husk, J. Colloid Interface Sci. (2005) https://doi.org/10.1016/j.jcis.2005.01.007.

[35] Y. Bulut, H. Aydin, A kinetics and thermodynamics study of methylene blue adsorption on wheat shells, Desalination (2006)https://doi.org/10.1016/j.desal.2005.10.032.

[36] B.G. Saucedo-Delgado, D.A. De Haro-Del Rio, L.M. González-Rodríguez, H.E. Reynel-Ávila, D.I. Mendoza-Castillo, A. Bonilla-Petriciolet, J. Rivera de la Rosa, Fluoride adsorption from aqueous solution using a protonated clinoptilolite and its modeling with artificial neural network-based equations, J. Fluor. Chem. (2017)https://doi.org/10.1016/j.jfluchem.2017.11.002.

[37] S. Hong, C. Wen, J. He, F. Gan, Y.S. Ho, Adsorption thermodynamics of methylene blue onto bentonite, J. Hazard. Mater. (2009)https://doi.org/10.1016/j.jhazmat.2009.01.014.

[38] N. Soltani, E. Saion, M.Z. Hussein, M. Erfani, A. Abedini, G. Bahmanrokh, M. Navasery, P. Vaziri, Visible light-induced degradation of methylene blue in the presence of photocatalytic ZnS and CdS nanoparticles, Int. J. Mol. Sci. (2012)https://doi.org/10.3390/ijms131012242.

[39] K.S.W. Sing, R.T. Williams, Physisorption hysteresis loops and the characterization of nanoporous materials, Adsorpt. Sci. Technol. (2004)https://doi.org/10.1260/0263617053499032.

[40] M. Onal, Physicochemical properties of bentonites: an overview, Commun. Fac. Sci. Univ. Ank. Ser. B. (2006)https://doi.org/10.1501/Commub_0000000349.

[41] S. Yang, D. Zhao, H. Zhang, S. Lu, L. Chen, X. Yu, Impact of environmental conditions on the sorption behavior of Pb(II) in Na-bentonite suspensions, J. Hazard. Mater. (2010)https://doi.org/10.1016/j.jhazmat.2010.07.072.

[42] Methylene Blue Spectrum, https://sdbs.db.aist.go.jp/sdbs/cgi-bin/IMG.cgi?imgdir=ir&fname=NIDA6365&sdbsno=2609, Accessed date: 21 December 2018.